

# An inverse model for injection molding of optical lens using artificial neural network coupled with genetic algorithm

Kuo-Ming Tsai · Hao-Jhih Luo

Received: 20 May 2014 / Accepted: 6 November 2014 / Published online: 15 November 2014  
© Springer Science+Business Media New York 2014

**Abstract** This study combined the artificial neural network (ANN) with a genetic algorithm (GA) to establish an inverse model of injection molding for optical lens form accuracy. The Taguchi parameter design was used for screening experiments of the injection molding parameters, and the significant factors influencing lens form accuracy were found to be mold temperature, cooling time, packing pressure, and packing time. These significant factors were used for full factorial experiments, and the experimental data then were used as training and checking data sets for the ANN prediction model. Finally, the ANN prediction model was combined with the GA to construct an inverse model of injection molding. Lens form accuracies of 0.5, 0.7, and 1  $\mu\text{m}$  were taken as examples for validation, and when the error of the set lens form accuracy target value was within 2% there were 26, 17, and six sets of the injection molding parameters, respectively, that met the desired form accuracy obtained by using the inverse model. The result indicated that the proposed strategy was successful in identifying process parameters for products with reliable accuracy. In addition, using the GA as a global search algorithm for the optimal solution could further optimize the Taguchi optimal process parameters. The validation experiments revealed that the form accuracy of the lens was improved.

**Keywords** Inverse model · Artificial neural network (ANN) · Genetic algorithm (GA) · Injection molding · Optical lens · Taguchi method

## Introduction

Plastics have better characteristics than general traditional industrial materials. These characteristics, such as a low density, corrosion resistance, workability, and low prices, have caused plastic products to increasingly be used as a substitute for metal and glass wares. In recent years, with the rapid development of electro-optical and information technology industries, the demand for various optical elements and photovoltaic systems has greatly increased. Optical lenses are indispensable components of these systems. The common methods used for producing plastic goods include injection molding, compression molding, blow molding, extrusion molding, and co-injection molding. The injection molding method is characterized by high productivity and yield, making it feasible for automation and the production of parts with complicated shapes. The injection molding process can be divided into several stages according to the operating cycles, including plastication, filling, packing, cooling and ejection. First, plastic pellets are plasticized into melt after screw shearing and feed pipe heating. Then, the melt is injected into the runner system of the mold to fill the cavities. Finally, the finished product is ejected after cooling. During the injection molding process, the melt is a non-Newtonian fluid with complex and highly nonlinear material characteristics. The temperature, shear rate, velocity, and pressure in the injection molding process can influence the quality of the final molded products. Building the prediction models, such as the artificial neural network (ANN) model to predict warpage (Yen et al. 2006), shrinkage (Altan 2010), flash (Zhu and Chen 2006), short shot and weld line (Sadeghi 2000), thickness reduction and porosity creation (Kwak et al. 2005), and weight and length (Chen et al. 2009b), as well as a regression model to predict warpage (Chen et al. 2009a) and a response surface methodology (RSM) model to predict weld line (Ozcelik and

---

K.-M. Tsai (✉) · H.-J. Luo  
Department of Mechanical Engineering, National Chin-Yi University of Technology, Taichung, Taiwan, Republic of China  
e-mail: tsai101@ncut.edu.tw

Erzurumlu 2005; Ozcelik 2011), in order to master the correlation between process parameters and the quality of molded products, are effective solutions. Many researchers have used different optimization approaches to obtain the optimal injection molding parameters, such as genetic algorithms (GA) to minimize warpage (Ozcelik and Erzurumlu 2005; Yin et al. 2011), particle swarm optimization (PSO) to minimize product and mold costs (Che 2010) and optimize product quality (Katherasan et al. 2014), the hybrid adaptive network based fuzzy inference system (ANFIS) with a multi-input multi-output (MIMO) strategy to optimize product quality (Huang and Chang 2011), hybrid ANN/GA to minimize shrinkage (Shen et al. 2007) and warpage (Yin et al. 2011), combined design of experiment (DOE)/ANN/GA to minimize warpage (Ozcelik and Erzurumlu 2005, 2006; Kurtaran et al. 2005), as well as research and applications regarding quality monitoring (Chen and Turg 2005; Lau et al. 2005; Li et al. 2009). The use of different optimization methods to obtain a prediction model for products is called forward modeling.

During molding trials, the operator will set up an initial process point based on his experience. This procedure depends on many factors, such as the molding material, the part geometry, the mold layout, and the molding machine. The process parameters will be adjusted repeatedly until the molding trial fully and successfully satisfies the quality of the molded parts. Parameter setting is a highly skilled job that is based on the skilled operator's "know-how" and intuitive sense acquired through long-term experience rather than through a theoretical and analytical approach. However, in a globally competitive industry such as injection molding, it is no longer enough to use the experience approach to determine the process parameters for injection molding. Typically, the inverse problem for injection molding is used to determine the process parameters for producing products with the desired quality values. A number of researchers have attempted various approaches to facilitate injection molding process setups that can reduce the time to market and obtain consistent quality products (Mok et al. 1999), such as fuzzy (Li et al. 2009), fuzzy-ANN (He et al. 1998; Mok and Kwong 2002; Huang and Chang 2011), fuzzy-GA (Lau et al. 2005), ANN-GA (Mok et al. 2001; Chen et al. 2009b), intelligent hybrid systems based on ANN-GA (Mok et al. 2000), data envelopment analysis (DEA) (Loera et al. 2008), and simplex (Kamoun et al. 2009). By using these methods, a set of process parameters can be determined, either on-line or off-line, to produce a near-optimal quality product. In reality, however, multiple sets of process parameters can be identified for near-optimal quality products.

The precision requirement for plastic optical lenses is higher than that for general plastic molded products, and if the molded lens profile is excessively deviated from the design value, the optical properties of the lens will be deteriorated and even unworkable. Therefore, this study investi-

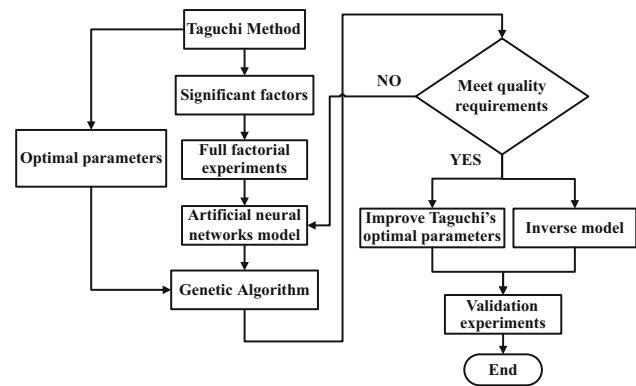


Fig. 1 Flow chart for this study

gated the form accuracy of a plastic optical lens and proposed a process parameter optimization model for injection molding, in which the most appropriate process parameters were inversely obtained according to the demand for form accuracy of optical lenses, in order to allow operators to rapidly obtain the appropriate process parameters needed to deliver the required product quality. A hybrid DOE, ANN and GA modeling approach was presented, from which several sets of process parameters could be quickly determined. To validate the feasibility of the approach, a case study on setting the processing parameters in injection molding was conducted, with promising results.

### Optimization strategy

A hybrid DOE, ANN and GA approach was developed to determine the sets of process parameters meeting the desired lens form accuracy. The overall procedure was as shown in Fig. 1. Taguchi experiments were used to identify the significant factors affecting the form precision of the lens for the injection molding process, as well as to determine the optimal parameters. The significant factors were then used to implement a full factorial experiment, and the experimental data were used to establish the ANN prediction model for form accuracy of the lens. Finally the trained ANN model was combined with a GA to establish the reverse model for injection molding and to identify multiple sets of process parameters for producing lenses with the desired form accuracy. The ANN and GA models were also used to improve the optimal parameters obtained from the Taguchi method. Confirmation experiments were performed to verify the accuracy of the hybrid model.

### Taguchi method

The qualities of the molded parts for injection molding are affected by a number of process parameters. This study inves-

tingated the form accuracy of a spherical lens using a Taguchi experiment to identify significant influencing factors. The form accuracy of a lens is a Smaller-the-Better (STB) quality characteristic. The signal to noise ratio (S/N ratio) of the STB is defined (Montgomery 2001; Taguchi et al. 2005) as:

$$S/N = -10 \log_{10} \left( \frac{1}{n} \sum_{i=1}^n y_i^2 \right) \text{ (dB)} \tag{1}$$

After the significant factors were identified, a series of confirmation experiments using the optimized parameter were subsequently performed. The successful confirmation experiments indicated that the set of significant factors obtained were valid and that the Taguchi method was applicable. If the confirmation result failed, the set of factors that had been selected earlier would be considered inadequate; consequently, the procedures would be repeated. In order to simply the process, the authors used an L<sub>18</sub>(2<sup>1</sup> × 3<sup>7</sup>) array in this study.

### Neural network

The artificial neural network (ANN) is a parallel computational model that is similar to the biological neural mechanism, namely, using computer calculations to simulate a human cerebral nerve cell network. The back-propagation neural network (BPNN) is one of the most representative and popular neural network among numerous neural networks (Ozcelik 2011; Katherasan et al. 2014; Ashhab et al. 2014). BPNN is a multilayer feedforward network that uses a supervised learning method to handle the nonlinear relations between the input and output variables. This study used a three-layer BPNN with a hidden layer to build an optical lens form accuracy prediction model. The output of each neuron is calculated based on the sum of the weights of all the connected nodes from the preceding layer plus a bias, and the activation function generates an output according to the following:

$$net_i = \sum_{j=0}^n w_{ij}x_j + b_{oi} \tag{2a}$$

$$Y_i = f(net_i) \tag{2b}$$

where,  $net_i$  is the aggregation function of the  $i$ th neuron in the layer,  $n$  denotes the number of neurons,  $w_{ij}$  is the associated weight between the  $i$ th and  $j$ th neurons,  $x_j$  represents the output of the  $j$ th neuron, and  $b_{oi}$  is the bias weight on the  $i$ th neuron and output of the  $i$ th neuron in the computing layer.  $Y_i = f(net_i)$  is generated by processing the input ( $net_i$ ) through an activation function.

The activation function for the hidden layer and are output layer of the network are a positive logarithmic sigmoid

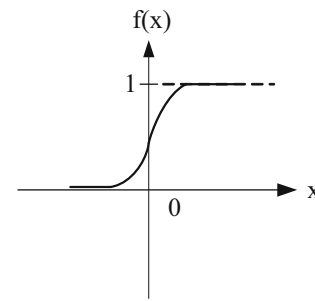


Fig. 2 Positive logistic function

function, and the input–output relationship is:

$$f(net_i) = \frac{1}{1 + e^{-(\lambda net_i)}} \tag{3}$$

where,  $\lambda$  is the gain factor of the neurons. The value of this activation function approaches 0 and 1, respectively, when the independent variable approaches plus-minus infinity, as shown in Fig. 2.

In the process of training the neural network of this study, the performance function was represented by the mean square error (MSE), i.e. the average of the square errors between the neural network inference value and the target value, defined as follows:

$$MSE = \frac{1}{n} \sum_{i=1}^n (T_i - A_i)^2 \tag{4}$$

where  $T_i$  is the target value of the  $i$ th training data or checking data,  $A_i$  is the network inference value of the  $i$ th training data or checking data, and  $n$  is the number of training data or checking data.

### Genetic algorithm (GA)

The genetic algorithm is an optimization method based on the Darwinian fitness. The basic mathematical units of the GA include the chromosomes, population size, bit length, and fitness function, as well as the three major operating mechanisms of selection (reproduction), crossover, and mutation, which are used to imitate the process of organic evolution. The GA is an algorithm for the global search of optimal solutions (Ozcelik 2011). In this study, the implementation of the GA consisted of the following four parts: (1) encoding, (2) fitness function, (3) selection mechanism, and (4) crossover and mutation mechanism. The parameters for the GA were encoded by binary encoding into strings of 0 and 1, and the initial population was randomly generated.

In a GA, a fitness function as an objective function can be designed according to different problems and demands, and the optimal solution is searched for according to a pre-

set range of parameters. This study used the trained ANN prediction model for the fitness function. Since the goal output of an ANN prediction model is normalized, the values are between 0 and 1, whereas the GA generally searches the maximum value of a system. Therefore, subtracting a predefined positive integer with the prediction value of the ANN model transforms the system into a minimizing problem. The searching range for the fitness function of the GA is typically the domain of the operating parameters of a machine; in this study the Taguchi optimal parameter values  $\pm 20\%$  were taken as the GA searching range to increase computation efficiency. Two fitness functions were defined and used to optimize the process parameters for injection molding, as follows:

1. Fitness function for inverse calculation of the process parameters  
Minimize:

$$obj = 1 - |PV - A| \quad (5)$$

Subject to:

The optimal values of the four significant factors identified by the Taguchi method  $\pm 20\%$ .

where *obj* is the fitness function, *PV* is the specified value of the lens form accuracy, and *A* is the inference value of the trained ANN model.

2. Fitness function for improvement of Taguchi optimal parameters  
Minimize:

$$obj = 1 - A \quad (6)$$

Subject to:

The optimal values of the four significant factors identified by the Taguchi method,  $\pm 20\%$ .

In this study, the GA was used to determine the appropriate parameter sets meeting the desired form accuracy of the lens. The optimal process parameters obtained from the Taguchi method were assigned to the baseline (initial population).

#### Coefficient of determination

In the ANN model, in order to express the fitness of the model for experimental data, the coefficient of determination ( $R^2$ ) is often used to determine the accuracy of the model. The larger the  $R^2$  is, the higher the fitness will be, i.e., the closer the model prediction value will be to the experimental value.  $R^2$  is defined (Montgomery 2001) as:

$$R^2 = \frac{\text{Regression sum of squares (SSR)}}{\text{Total sum of squares (SST)}}$$

$$= 1 - \frac{\text{Error sum of squares (SSE)}}{\text{Total sum of squares (SST)}} \quad (7)$$

where, SST (total sum of squares) is the total variance, SSR (regression sum of squares) is the amount of variation that can be explained by the model, and SSE (error sum of squares) is the amount of random variation that cannot yet be explained by the model.

## Experimental setup

This study combined ANN and GA to establish an inverse model of injection molding, and two experiments were conducted. The first experiment was the Taguchi experiment, which screened out the significant factors influencing lens form accuracy and obtained the Taguchi optimal parameters, and the second experiment was a full factorial experiments based on significant factors. The second experimental data was used to establish the ANN prediction model for lens form accuracy.

#### Experimental equipment and material

This study used an injection molding machine and various measuring instruments. A 220S 250-60 precision injection molding machine produced by Arburg (Germany) was used for the injection molding experiments, and the surface form accuracy of the lens was measured via a Form Talysurf PGI-840 surface contour profilometer made by Taylor Hobson (Britain). The ANN and GA programs for form accuracy data used MATLAB<sup>®</sup> software with neural network Toolbox (R2012b). The experimental material was optical grade PMMA-80N (polymethyl methacrylate), manufactured by Asahi Kasei (Japan). Five specimens were sampled at the same cavity of the four-cavity mold, and the average value was taken as the experimental data.

#### Experimental mold

A plano-convex lens was adopted, as shown in Fig. 3a, and a four-cavity layout of the product was designed in a mold, as shown in Fig. 3b. The diameter of the lens was 15 mm, the effective spherical diameter of the lens was 13 mm and the maximum thickness at the lens center was 1.4243 mm.

## Results and discussion

#### Significant factors

The Taguchi parameter design used an  $L_{18}(2^1 \times 3^7)$  orthogonal array. The eight control factors were melt tempera-

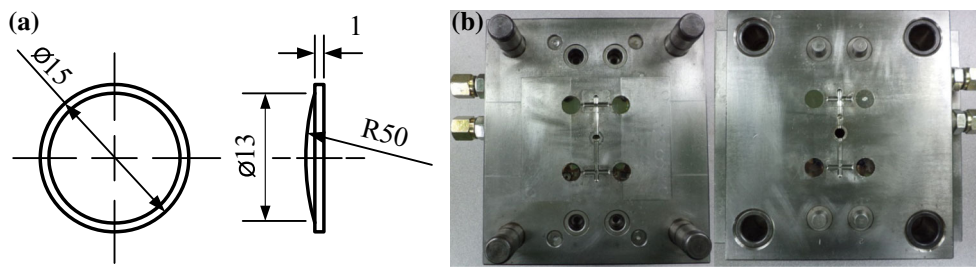


**Fig. 3** Dimensions of the plano-convex lens. **a** Dimensions of the lens. **b** Part layout in the mold

**Table 1** Factors and levels for the Taguchi experiment

| Control factor               | Level 1 | Level 2 | Level 3 |
|------------------------------|---------|---------|---------|
| A. Melt temperature (°C)     | 230     | 240     |         |
| B. Injection velocity (mm/s) | 80      | 90      | 100     |
| C. Injection pressure (MPa)  | 90      | 100     | 110     |
| D. VP switch over (mm)       | 6.12    | 6.24    | 6.36    |
| E. Packing time (s)          | 5       | 7       | 9       |
| F. Packing pressure (MPa)    | 100     | 110     | 120     |
| G. Mold temperature (°C)     | 70      | 85      | 100     |
| H. Cooling time (s)          | 15      | 20      | 25      |

ture, injection speed, injection pressure, filling to packing switchover position, packing pressure, packing time, mold temperature, and cooling time. The factor levels are shown in Table 1. The experimental result is shown in Table 2, in which the lens form accuracies were the average value

of five parts. The response graph in Fig. 4 was obtained according to the S/N ratio of the STB characteristic. It was observed that the optimal parameter levels combination was A<sub>2</sub>B<sub>2</sub>C<sub>3</sub>D<sub>3</sub>E<sub>2</sub>F<sub>2</sub>G<sub>2</sub>H<sub>3</sub>, i.e., a melt temperature of 240 °C, an injection speed of 90 mm/s, an injection pressure of 110 MPa, a filling to packing switchover position of 6.36 mm, a packing pressure of 110 MPa, a packing time of 7 s, a mold temperature of 85 °C and a cooling time of 25 s.

Analysis of variance (ANOVA) is usually used to identify the influence of control factors. Table 3 is the ANOVA table of the lens form accuracy S/N ratio, which shows that the most significant influence factor was the mold temperature. In addition, according to the contribution rate, four control factors were selected for 3<sup>4</sup> full factorial experiments to obtain learning and testing data for the ANN model. The factors included mold temperature, cooling time, packing pressure and packing time.

**Table 2** Form accuracies and S/N ratio for L<sub>18</sub>(2<sup>1</sup> × 3<sup>7</sup>)

| Run | Control factor |   |   |   |   |   |   |   |   | Experiment | S/N (dB) |
|-----|----------------|---|---|---|---|---|---|---|---|------------|----------|
|     | A              | B | C | D | E | F | G | H |   |            |          |
| 1   | 1              | 1 | 1 | 1 | 1 | 1 | 1 | 1 | 1 | 0.829      | 1.63     |
| 2   | 1              | 1 | 2 | 2 | 2 | 2 | 2 | 2 | 2 | 0.603      | 4.39     |
| 3   | 1              | 1 | 3 | 3 | 3 | 3 | 3 | 3 | 3 | 0.958      | 0.37     |
| 4   | 1              | 2 | 1 | 1 | 2 | 2 | 3 | 3 |   | 0.833      | 1.59     |
| 5   | 1              | 2 | 2 | 2 | 3 | 3 | 1 | 1 |   | 0.697      | 3.14     |
| 6   | 1              | 2 | 3 | 3 | 1 | 1 | 2 | 2 |   | 0.571      | 4.87     |
| 7   | 1              | 3 | 1 | 2 | 1 | 3 | 2 | 3 |   | 0.647      | 3.78     |
| 8   | 1              | 3 | 2 | 3 | 2 | 1 | 3 | 1 |   | 1.018      | -0.15    |
| 9   | 1              | 3 | 3 | 1 | 3 | 2 | 1 | 2 |   | 0.565      | 4.96     |
| 10  | 2              | 1 | 1 | 3 | 3 | 2 | 2 | 1 |   | 0.555      | 5.11     |
| 11  | 2              | 1 | 2 | 1 | 1 | 3 | 3 | 2 |   | 1.203      | -1.61    |
| 12  | 2              | 1 | 3 | 2 | 2 | 1 | 1 | 3 |   | 0.566      | 4.94     |
| 13  | 2              | 2 | 1 | 2 | 3 | 1 | 3 | 2 |   | 1.088      | -0.73    |
| 14  | 2              | 2 | 2 | 3 | 1 | 2 | 1 | 3 |   | 0.554      | 5.13     |
| 15  | 2              | 2 | 3 | 1 | 2 | 3 | 2 | 1 |   | 0.632      | 3.99     |
| 16  | 2              | 3 | 1 | 3 | 2 | 3 | 1 | 2 |   | 0.683      | 3.31     |
| 17  | 2              | 3 | 2 | 1 | 3 | 1 | 2 | 3 |   | 0.553      | 5.15     |
| 18  | 2              | 3 | 3 | 2 | 1 | 2 | 3 | 1 |   | 1.049      | -0.42    |

**Fig. 4** Response graph of S/N ratio for the form accuracy of the lenses

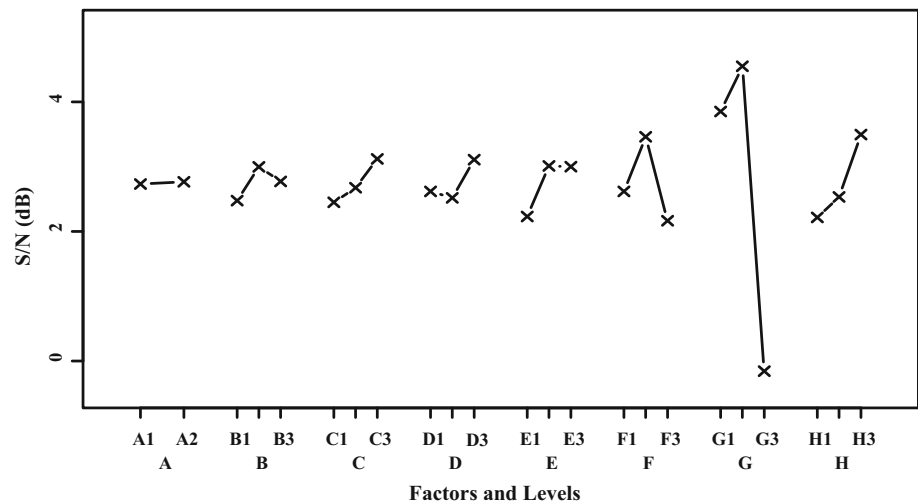


**Table 3** Analysis of variance for S/N ratio

| Factors     | SS       | DF   | MS       | F value | Contr. rate (%) |
|-------------|----------|------|----------|---------|-----------------|
| A           | 0.0047   | 1    | 0.0047   | *       | 0.005           |
| B           | 0.8375   | 2    | 0.4188   | *       | 0.884           |
| C           | 1.3936   | 2    | 0.6968   | *       | 1.471           |
| D           | 1.1938   | 2    | 0.5969   | *       | 1.260           |
| E           | 2.4081   | 2    | 1.2040   | *       | 2.541           |
| F           | 5.1935   | 2    | 2.5968   | 4.1837  | 5.480           |
| G           | 77.4363  | 2    | 38.7182  | 62.3783 | 81.714          |
| H           | 5.3078   | 2    | 2.6539   | 4.2757  | 5.601           |
| Residual    | 0.9902   | 2    | 0.4951   |         | 1.045           |
| (Residuals) | (6.8279) | (11) | (0.6207) |         |                 |
| Total       | 94.7656  | 17   |          |         | 100             |

$F_{(0.05,2,11)} = 3.98$

\* The terms are not significant and can be merged to residuals

The optimal parameter level combination could be obtained by the Taguchi experiment. However, the results needed to be experimentally verified because the number of Taguchi experiments was too small. In the  $L_{18}$  Taguchi experiments, the average value of the S/N ratio was 2.75 dB. Based on the significant factors in ANOVA, i.e., the four control factors listed above, the predicted value of the S/N ratio of the optimal conditions was estimated as:

$$\begin{aligned}
 \hat{\eta} &= \bar{T} + (F_2 - \bar{T}) + (G_2 - \bar{T}) + (H_3 - \bar{T}) \\
 &= F_2 + G_2 + H_3 - 2 \times \bar{T} \\
 &= 3.46 + 4.55 + 3.49 - 2 \times 2.75 \\
 &= 6 \text{ (dB)}
 \end{aligned} \tag{8}$$

An important step in the Taguchi optimization technique is conducting a confirmation experiment to validate the predicted result. The confidence interval (CI) is the maximum and minimum value between which the true value should fall at some stated percentage of confidence. The 95% confidence interval for the predicted value of the optimal parameter level combination on a confirmation test can be calculated by the

following equation (Ross 1996; Chaulia and Das 2008; Tang et al. 2013). In this work, the optimal condition was used for five confirmation experiments to calculate CI, in which  $F_{0.05,1,11} = 4.84$ . From the ANOVA Table,  $V_e = 0.6207$  and  $r = 5$ , and then:

$$\begin{aligned}
 CI_{SN} &= \sqrt{F_{\alpha;v_1,v_2} \times V_e \times \left( \frac{1}{n_{eff}} + \frac{1}{r} \right)} \\
 &= \sqrt{4.84 \times 0.6207 \times \left( \frac{1}{2.571} + \frac{1}{5} \right)} \\
 &= 1.33 \text{ (dB)}
 \end{aligned} \tag{9}$$

where,  $F_{\alpha;v_1,v_2}$  denotes the F value of  $\alpha$  at a level of significance, the level of confidence is  $1 - \alpha$ ,  $v_1$  is the degree of freedom (DF) for the mean which is always = 1,  $v_2$  denotes the DF of the pooled error variance,  $V_e$  is the pooled error variance,  $n_{eff}$  is the number of effective experimental values, and  $r$  is the number of replication for confirmation experiments.

**Table 4** The result of the Taguchi confirmation experiments

| Optimal parameters |         | A <sub>2</sub> B <sub>2</sub> C <sub>3</sub> D <sub>3</sub> E <sub>2</sub> F <sub>2</sub> G <sub>2</sub> H <sub>3</sub> |       |       |       |       |
|--------------------|---------|---|-------|-------|-------|-------|
| Prediction         | S/N     | 6 ± 1.33 (4.67–7.33) dB   |       |       |       |       |
| Experiment         | PV (μm) | 0.509   | 0.465 | 0.491 | 0.461 | 0.473 |
|                    | S/N     | 5.87  | 6.65  | 6.18  | 6.73  | 6.50  |

$$n_{\text{eff}} = \frac{\text{Total run of experiments (N)}}{1 + \text{Degree of freedom for significant factors (DF)}} = \frac{18}{1 + (2 + 2 + 2)} = 2.571 \quad (10)$$

The predicted S/N ratio of the optimal process parameters was 6 ± 1.33 dB (4.67–7.33 dB). The results of the five validation experiments are shown in Table 4. It was observed that the S/N ratios of all experimental runs were within the confidence interval, proving that the Taguchi experiment result was reliable.

ANN learning data set experiments

This study used four significant factors, including mold temperature, cooling time, packing pressure, and packing time, for the full factorial experiments. According to the aforesaid S/N ratio response graph of lens form accuracy, the longer the cooling time, the better the form accuracy would be. Therefore, in order to obtain better lens form accuracy, the range of the cooling time was reset as 20–30 s. The levels for the mold temperature, packing pressure, and packing time were maintained as in the range of the Taguchi experiment, and the other fixed injection molding parameters used the optimal process parameters obtained from the Taguchi experiment. The factor levels of 3<sup>4</sup> full factorial experiments are shown in Table 5. A total of 81 experimental runs were implemented, and the results were as shown in Table 6, in which 60 groups were the training data sets for learning the neural network model, and the remaining 21 groups were the testing data sets.

**Table 5** Factors and levels for the 3<sup>4</sup> full factorial experiments

| Control factor            | Value |     |     |
|---------------------------|-------|-----|-----|
| Melt temperature (°C)     | 240   |     |     |
| Injection velocity (mm/s) | 90    |     |     |
| Injection pressure (MPa)  | 110   |     |     |
| VP switch over (mm)       | 6.36  |     |     |
| Packing time (s)          | 5     | 7   | 9   |
| Packing pressure (MPa)    | 100   | 110 | 120 |
| Mold temperature (°C)     | 70    | 85  | 100 |
| Cooling time (s)          | 20    | 25  | 30  |

**Table 6** Form accuracy of the lenses for the 3<sup>4</sup> experiments

| Run             | Mold temp | Packing press | Packing time | Cooling time | PV (μm) | σ     |
|-----------------|-----------|---------------|--------------|--------------|---------|-------|
| 1               | 70        | 100           | 5            | 20           | 0.711   | 0.064 |
| 2               | 70        | 100           | 5            | 25           | 0.692   | 0.069 |
| 3               | 70        | 100           | 5            | 30           | 0.761   | 0.099 |
| 4 <sup>a</sup>  | 70        | 100           | 7            | 20           | 0.541   | 0.051 |
| 5               | 70        | 100           | 7            | 25           | 0.542   | 0.081 |
| 6               | 70        | 100           | 7            | 30           | 0.595   | 0.102 |
| 7               | 70        | 100           | 9            | 20           | 0.615   | 0.082 |
| 8 <sup>a</sup>  | 70        | 100           | 9            | 25           | 0.562   | 0.055 |
| 9               | 70        | 100           | 9            | 30           | 0.528   | 0.043 |
| 10              | 70        | 110           | 5            | 20           | 0.587   | 0.029 |
| 11              | 70        | 110           | 5            | 25           | 0.515   | 0.026 |
| 12 <sup>a</sup> | 70        | 110           | 5            | 30           | 0.589   | 0.055 |
| 13              | 70        | 110           | 7            | 20           | 0.572   | 0.072 |
| 14              | 70        | 110           | 7            | 25           | 0.651   | 0.067 |
| 15              | 70        | 110           | 7            | 30           | 0.594   | 0.02  |
| 16 <sup>a</sup> | 70        | 110           | 9            | 20           | 0.510   | 0.056 |
| 17              | 70        | 110           | 9            | 25           | 0.475   | 0.028 |
| 18              | 70        | 110           | 9            | 30           | 0.536   | 0.038 |
| 19              | 70        | 120           | 5            | 20           | 0.712   | 0.058 |
| 20 <sup>a</sup> | 70        | 120           | 5            | 25           | 0.614   | 0.079 |
| 21              | 70        | 120           | 5            | 30           | 0.510   | 0.031 |
| 22              | 70        | 120           | 7            | 20           | 0.640   | 0.068 |
| 23              | 70        | 120           | 7            | 25           | 0.610   | 0.074 |
| 24 <sup>a</sup> | 70        | 120           | 7            | 30           | 0.503   | 0.059 |
| 25              | 70        | 120           | 9            | 20           | 0.523   | 0.052 |
| 26              | 70        | 120           | 9            | 25           | 0.457   | 0.023 |
| 27 <sup>a</sup> | 70        | 120           | 9            | 30           | 0.574   | 0.078 |
| 28              | 85        | 100           | 5            | 20           | 0.511   | 0.035 |
| 29              | 85        | 100           | 5            | 25           | 0.521   | 0.061 |
| 30              | 85        | 100           | 5            | 30           | 0.503   | 0.041 |
| 31 <sup>a</sup> | 85        | 100           | 7            | 20           | 0.492   | 0.05  |
| 32              | 85        | 100           | 7            | 25           | 0.486   | 0.035 |
| 33              | 85        | 100           | 7            | 30           | 0.513   | 0.02  |
| 34              | 85        | 100           | 9            | 20           | 0.523   | 0.04  |
| 35 <sup>a</sup> | 85        | 100           | 9            | 25           | 0.514   | 0.029 |
| 36              | 85        | 100           | 9            | 30           | 0.500   | 0.021 |
| 37              | 85        | 110           | 5            | 20           | 0.589   | 0.059 |
| 38              | 85        | 110           | 5            | 25           | 0.509   | 0.031 |
| 39 <sup>a</sup> | 85        | 110           | 5            | 30           | 0.471   | 0.029 |
| 40              | 85        | 110           | 7            | 20           | 0.453   | 0.019 |
| 41              | 85        | 110           | 7            | 25           | 0.463   | 0.016 |
| 42              | 85        | 110           | 7            | 30           | 0.475   | 0.033 |
| 43 <sup>a</sup> | 85        | 110           | 9            | 20           | 0.514   | 0.038 |
| 44              | 85        | 110           | 9            | 25           | 0.534   | 0.041 |
| 45              | 85        | 110           | 9            | 30           | 0.516   | 0.021 |
| 46              | 85        | 120           | 5            | 20           | 0.576   | 0.071 |

**Table 6** continued

| Run             | Mold temp | Packing press | Packing time | Cooling time | PV ( $\mu\text{m}$ ) | $\sigma$ |
|-----------------|-----------|---------------|--------------|--------------|----------------------|----------|
| 47 <sup>a</sup> | 85        | 120           | 5            | 25           | 0.549                | 0.034    |
| 48              | 85        | 120           | 5            | 30           | 0.516                | 0.057    |
| 49              | 85        | 120           | 7            | 20           | 0.445                | 0.025    |
| 50              | 85        | 120           | 7            | 25           | 0.496                | 0.033    |
| 51 <sup>a</sup> | 85        | 120           | 7            | 30           | 0.489                | 0.027    |
| 52              | 85        | 120           | 9            | 20           | 0.498                | 0.018    |
| 53              | 85        | 120           | 9            | 25           | 0.552                | 0.074    |
| 54 <sup>a</sup> | 85        | 120           | 9            | 30           | 0.487                | 0.035    |
| 55              | 100       | 100           | 5            | 20           | 0.666                | 0.046    |
| 56              | 100       | 100           | 5            | 25           | 0.748                | 0.053    |
| 57              | 100       | 100           | 5            | 30           | 0.792                | 0.014    |
| 58 <sup>a</sup> | 100       | 100           | 7            | 20           | 0.989                | 0.067    |
| 59              | 100       | 100           | 7            | 25           | 0.941                | 0.039    |
| 60              | 100       | 100           | 7            | 30           | 1.004                | 0.058    |
| 61              | 100       | 100           | 9            | 20           | 1.06                 | 0.062    |
| 62 <sup>a</sup> | 100       | 100           | 9            | 25           | 1.089                | 0.074    |
| 63              | 100       | 100           | 9            | 30           | 1.058                | 0.072    |
| 64              | 100       | 110           | 5            | 20           | 0.542                | 0.075    |
| 65              | 100       | 110           | 5            | 25           | 0.797                | 0.069    |
| 66 <sup>a</sup> | 100       | 110           | 5            | 30           | 0.861                | 0.047    |
| 67              | 100       | 110           | 7            | 20           | 0.886                | 0.046    |
| 68              | 100       | 110           | 7            | 25           | 1.019                | 0.051    |
| 69              | 100       | 110           | 7            | 30           | 1.006                | 0.086    |
| 70 <sup>a</sup> | 100       | 110           | 9            | 20           | 1.062                | 0.043    |
| 71              | 100       | 110           | 9            | 25           | 1.167                | 0.083    |
| 72              | 100       | 110           | 9            | 30           | 1.008                | 0.126    |
| 73              | 100       | 120           | 5            | 20           | 0.549                | 0.027    |
| 74 <sup>a</sup> | 100       | 120           | 5            | 25           | 0.707                | 0.036    |
| 75              | 100       | 120           | 5            | 30           | 0.79                 | 0.104    |
| 76              | 100       | 120           | 7            | 20           | 0.875                | 0.065    |
| 77              | 100       | 120           | 7            | 25           | 0.959                | 0.032    |
| 78 <sup>a</sup> | 100       | 120           | 7            | 30           | 0.996                | 0.075    |
| 79              | 100       | 120           | 9            | 20           | 0.991                | 0.047    |
| 80              | 100       | 120           | 9            | 25           | 1.054                | 0.071    |
| 81 <sup>a</sup> | 100       | 120           | 9            | 30           | 1.031                | 0.05     |

<sup>a</sup> Testing data set for ANN model fitting

### ANN model for quality prediction

The supervised BPNN model was constructed according to the 81 sets of full factorial experimental data as shown in Table 6, in which 60 groups were the training data sets and the remaining 21 groups were the testing data sets that determined the convergence step size, gradient direction, and stop learning of ANN. The training of this neural network model used the Levenberg–Marquardt algorithm with the gradient

**Table 7** Training variables for the back-propagation neural network

| Parameter        | Value |
|------------------|-------|
| Epochs           | 2,000 |
| Performance goal | 0     |
| Learning rate    | 0.01  |
| Gradient         | 1E–20 |

descent weight bias learning function, which has a higher network convergence rate. The other network training settings were as shown in Table 7.

The input variable of the BPNN was the significant factors influencing lens form accuracy, and the output variable was the lens form accuracy discussed in this study. A back-propagation multilayer neural network consists of three layers of neurons termed as the input, hidden, and output layers, as shown in Fig. 5. The flow chart of the learning and testing procedures for the proposed ANN model are shown in Fig. 6. The procedure was performed as an optimization algorithm. To obtain the optimal neural network, usually the number of neurons in the hidden layer is successively determined by experience or experimentation. In this study, an experiment was implemented to determine the number of hidden neurons. A neural network model of four to 12 neurons, at intervals of 2 neurons, was used to compare the coefficient of determination ( $R^2$ ) for the hidden layer. Simplistically, the experimental data sets shown in Table 6 were used to implement the training ANN model with a different number of neurons on the hidden layer. The results are shown in Table 8. According to the results, the larger the number of neurons, the smaller the MSE would be, and the lower the coefficient of determination. This is because the increase in the number of neurons resulted in overfitting, namely, in the training process, the error of the training data set was very small, while the error of the checking data set increased. In addition, the coefficient of determination of four neurons was better than that of six neurons; however, the MSE in the training process was larger, as shown in Fig. 7, which could result in a larger error in subsequent inverse modeling. Therefore, this study decided on six neurons in the hidden layer. The average error between the inference values of this ANN and the 21 test groups was 4.89%, and  $R^2$  was 0.9675.

### Inverse model

#### Hybrid ANN and GA

This study combined ANN with GA in order to construct an inverse model of the injection molding process. First, the process parameters were encoded into a binary format and the initial process parameters were randomly generated. The



Fig. 5 Architecture of the ANN

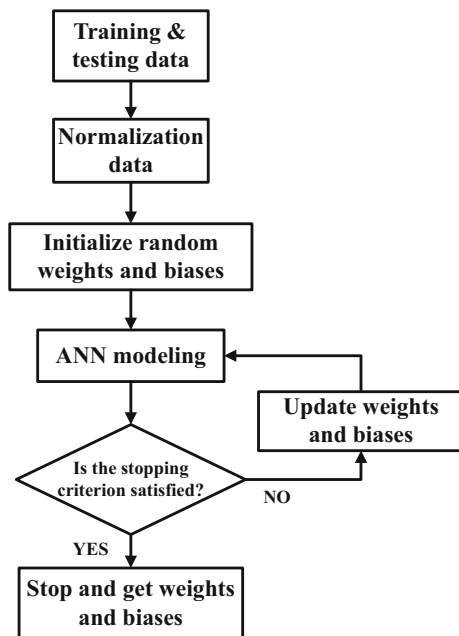
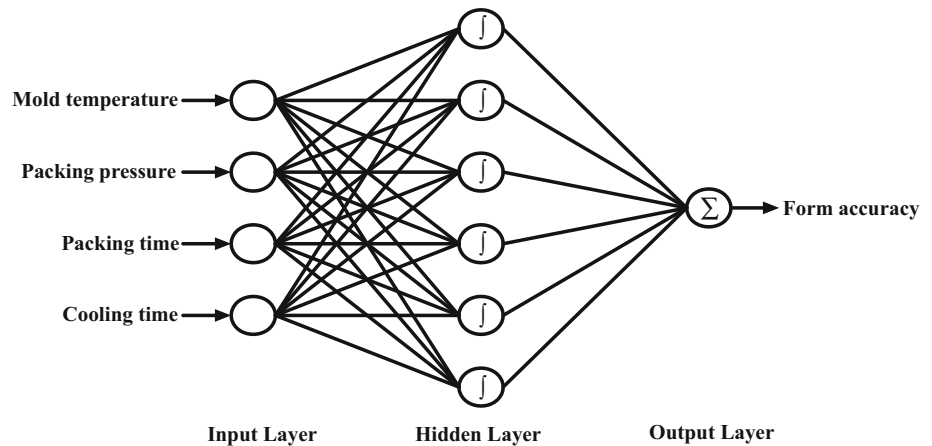


Fig. 6 Flow chart of the ANN learning and testing

above-trained ANN model for quality prediction was used to the fitness function of the GA, and the process parameters meeting the fitness function target were obtained through the evolutionary process of the GA. In the evolutionary process, parameters with higher fitness values were reserved in the next generation for crossover in order to obtain better process parameters, until the fitness value of the process parameters met the desired requirement and the optimal process parameters could be obtained.

The flow chart of the hybrid ANN and GA model is shown in Fig. 8. The required form accuracy of the lens was first assigned and the searching ranges for the four significant factors were determined. The data were then encoded and imported into the hybrid ANN and GA model. In this model, roulette wheel selection based on a ranking algorithm was used as the selection mechanism. Chromosomes were

Table 8 Comparison of different the number of hidden nodes

| Hidden nodes | Epochs | MSE (training) | R-square (checking) |
|--------------|--------|----------------|---------------------|
| 4            | 2,000  | 3.4E−04        | 0.9681              |
| 6            | 2,000  | 1.69E−04       | 0.9675              |
| 8            | 2,000  | 3.24E−05       | 0.9455              |
| 10           | 2,000  | 3.55E−06       | 0.9254              |
| 12           | 2,000  | 9.42E−07       | 0.8955              |

selected in quantities according to their relative fitness after ranking in the roulette wheel operator, and they were then fed into the intermediate population. The population size was 30. Single-point crossover and uniform mutation operators were used, and the probabilities of the crossover and mutation operators were 0.7 and 0.05, respectively. In addition, in the binary encoding of the process parameters in the GA, the string length of the genes determined the accuracy of the process parameter, i.e., the resolution. In terms of the packing pressure, the minimum resolution of the machine was set as 1 MPa, the search interval of the packing pressure was from 100 to 120 MPa, and the range of the GA parameters was obtained by broadening the upper and lower limits of the Taguchi optimal process parameters. The range is shown in Table 9. The string length was set as 5 in this study, meaning the range between 100 and 120 was divided into  $2^5$  equal parts. Each part was 0.625, which was lower than 1 MPa of the machine, and which met the optimization requirements. Therefore, the trained ANN model could precisely predict the form accuracy of lenses produced using the process parameters. The GA was then applied to obtain the robust process parameter settings for the investigated range.

Case study

According to the aforesaid results, mold temperature was the most significant factor influencing lens form accuracy.

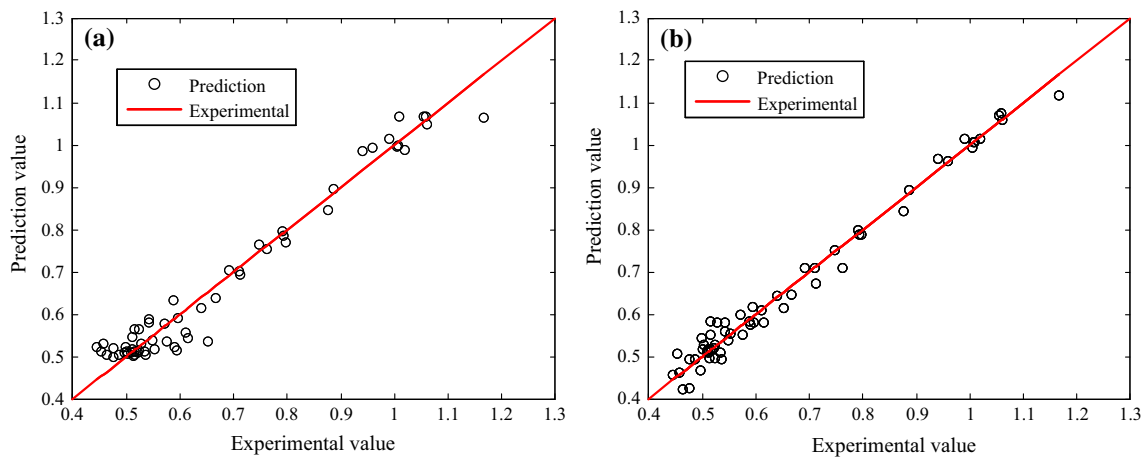


Fig. 7 Comparison of the prediction error at different hidden nodes. a Four hidden nodes. b Six hidden nodes

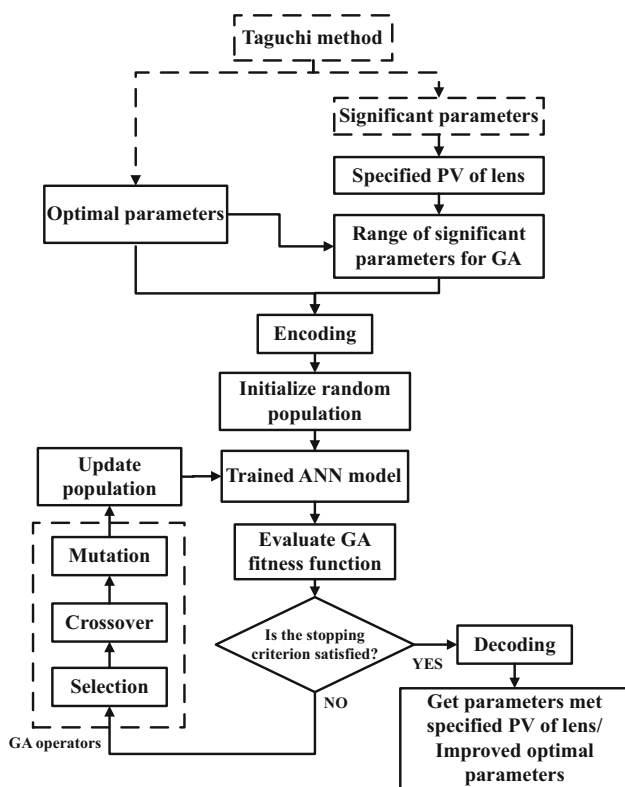


Fig. 8 Flow chart for the inverse model by hybrid ANN and GA

Therefore, the process parameters that met the form accuracy requirements at different mold temperatures could be obtained using the inverse model. This study took a form accuracy of 0.5, 0.7, and 1  $\mu\text{m}$ , respectively, as the examples, and used an ANN with a GA to develop the inverse model of the injection mold parameters. The fitness function of the GA used Eq. (5), within a targeted value of a 2% error, and consequently 26, 17, and 6 sets of the process parameters that met the quality requirements could be obtained by the proposed model, respectively. The details are shown in Tables 10, 11

Table 9 Variables for the genetic algorithm

| Parameter                               | Lower bound | Upper bound |
|---|-------------|-------------|
| Packing time (s)                        | 5           | 9           |
| Packing pressure (MPa)                  | 100         | 120         |
| Mold temperature ( $^{\circ}\text{C}$ ) | 70          | 100         |
| Cooling time (s)                        | 20          | 30          |
| Population size                         | 30          |             |
| Bit length                              | 5           |             |
| Generations                             | 500         |             |
| Crossover rate                          | 0.7         |             |
| Mutation rate                           | 0.02        |             |

and 12. The range of the process parameters was obtained, as shown in Table 13. When the form accuracy requirement was 1  $\mu\text{m}$ , there were only six sets of process parameters meeting the requirements, as the 1  $\mu\text{m}$  form accuracy could only be obtained if the mold temperature was higher than 95  $^{\circ}\text{C}$ .

In addition, the process parameters that met form accuracy requirements were drawn in three process parameter process windows. Figs. 9, 10 and 11 show the 3D process windows for a form accuracy of 0.5, 0.7, and 1  $\mu\text{m}$ , respectively. The points in the figures are the operating points where the desired form accuracy was obtained. The process window enabled the operators to see the range of process parameters that met the quality requirements, in order to rapidly select the process parameters with a shorter cooling time or lower mold temperature according to actual production requirements, such as shortening the production cycle time or reducing machine energy consumption. According to the process windows, the form accuracy of the lens deteriorated with an increasing mold temperature.

In order to verify the accuracy of the inverse models established by ANN with GA, some experimental conditions were selected at each mold temperature for the validation exper-

**Table 10** Parameters set of the process window at the form accuracy of 0.5 μm

| Mold temp. | Packing press. | Packing time | Cooling time | PV (μm) | Error (%) |
|------------|----------------|--------------|--------------|---------|-----------|
| 70         | 110            | 8.4          | 21.3         | 0.501   | 0.2       |
| 71         | 120            | 8.7          | 28.7         | 0.503   | 0.6       |
| 72         | 109            | 8.5          | 27.1         | 0.5     | 0         |
| 73         | 109            | 8.2          | 23.9         | 0.501   | 0.2       |
| 74         | 117            | 5.6          | 27.1         | 0.499   | 0.2       |
| 75         | 117            | 5.4          | 29           | 0.498   | 0.4       |
| 76         | 104            | 6.3          | 20.6         | 0.499   | 0.2       |
| 77         | 113            | 6.5          | 27.4         | 0.501   | 0.2       |
| 78         | 106            | 8.6          | 27.4         | 0.503   | 0.6       |
| 79         | 101            | 6.7          | 27.1         | 0.502   | 0.4       |
| 80         | 108            | 5.6          | 21.3         | 0.504   | 0.79      |
| 81         | 101            | 6.5          | 21.9         | 0.497   | 0.6       |
| 82         | 114            | 5.4          | 28.7         | 0.497   | 0.6       |
| 83         | 100            | 6.5          | 25.8         | 0.501   | 0.2       |
| 84         | 111            | 6.8          | 21           | 0.5     | 0         |
| 85         | 100            | 6.3          | 28.1         | 0.5     | 0         |
| 86         | 103            | 8.9          | 24.8         | 0.498   | 0.4       |
| 87         | 101            | 5.4          | 24.5         | 0.497   | 0.6       |
| 88         | 105            | 8.2          | 25.5         | 0.5     | 0         |
| 89         | 101            | 6.7          | 25.5         | 0.503   | 0.6       |
| 90         | 101            | 5.6          | 22.3         | 0.497   | 0.6       |
| 91         | 117            | 5.4          | 21           | 0.5     | 0         |
| 92         | 119            | 5.9          | 21.3         | 0.499   | 0.2       |
| 93         | 107            | 5.9          | 26.1         | 0.5     | 0         |
| 94         | 107            | 5.4          | 26.1         | 0.501   | 0.2       |
| 95         | 111            | 5            | 30           | 0.5     | 0         |
|            |                |              |              | Average | 0.3       |

iment. The error between the experimental values and the prediction values of the inverse models was calculated as follows:

$$\text{Error}(\%) = \left| \frac{\text{Experimental value} - \text{Predicted value}}{\text{Experimental value}} \right| \times 100\% \tag{11}$$

The results of experiments are shown in Table 14. The results showed that the maximum error between the experiment value and the prediction value for the model was 16.7 %, the smallest error was 2.63 %, and the average error was 8.27 %. Therefore, the inverse model via ANN with GA in this study demonstrated acceptable accuracy.

Improving the taguchi optimal process parameters

GA is capable of obtaining a global minimum value. This study was based on the Taguchi optimal process parameters,

**Table 11** Parameters set of the process window at the form accuracy of 0.7 μm

| Mold temp. | Packing press. | Packing time | Cooling time | PV(μm)  | Error (%) |
|------------|----------------|--------------|--------------|---------|-----------|
| 70         | 101            | 5            | 26.8         | 0.695   | 0.72      |
| 71         | 115            | 5.5          | 21           | 0.699   | 0.14      |
| 72         | 100            | 5            | 26.8         | 0.694   | 0.86      |
| 73         | 113            | 6.2          | 20           | 0.697   | 0.43      |
| 74         | 113            | 6.3          | 20           | 0.689   | 1.6       |
| 89         | 119            | 8.9          | 30           | 0.705   | 0.71      |
| 90         | 117            | 8.7          | 22.6         | 0.693   | 1.01      |
| 91         | 112            | 8.7          | 22.9         | 0.693   | 1.01      |
| 92         | 119            | 8.2          | 28.7         | 0.696   | 0.57      |
| 93         | 112            | 8.4          | 29.7         | 0.707   | 0.99      |
| 94         | 107            | 7.8          | 26.1         | 0.696   | 0.57      |
| 95         | 107            | 7.3          | 26.8         | 0.698   | 0.29      |
| 96         | 107            | 6.8          | 27.4         | 0.7     | 0         |
| 97         | 112            | 5.8          | 24.8         | 0.7     | 0         |
| 98         | 112            | 5.3          | 25.5         | 0.702   | 0.28      |
| 99         | 103            | 5.1          | 20           | 0.698   | 0.29      |
| 100        | 112            | 5.1          | 20.3         | 0.689   | 1.6       |
|            |                |              |              | Average | 0.65      |

**Table 12** Parameters set of the process window at the form accuracy of 1 μm

| Mold temp. | Packing press. | Packing time | Cooling time | PV (μm) | Error (%) |
|------------|----------------|--------------|--------------|---------|-----------|
| 95         | 103            | 9            | 20           | 0.991   | 0.91      |
| 96         | 117            | 9            | 29           | 1       | 0         |
| 97         | 111            | 8.2          | 27.1         | 0.998   | 0.2       |
| 98         | 101            | 8.4          | 27.4         | 1       | 0         |
| 99         | 114            | 7.7          | 22.6         | 0.997   | 0.3       |
| 100        | 105            | 8            | 26.1         | 0.998   | 0.2       |
|            |                |              |              | Average | 0.27      |

**Table 13** Process parameter ranges for different quality requirements

| PV (μm) | Mold temp. | Packing press. | Packing time | Cooling time |
|---------|------------|----------------|--------------|--------------|
| 0.5     | 70–95      | 100–120        | 5–8.9        | 20.6–30      |
| 0.7     | 70–74      | 100–115        | 5–6.3        | 20–26.8      |
|         | 89–100     | 103–119        | 5.1–8.9      | 20–30        |
| 1       | 95–100     | 101–117        | 7.7–9        | 20–29        |

which broadened the upper and lower bounds of 20 % for the process parameter range, and the optimal process parameters within the parameter limitation was obtained by the fitness function of Eq. (6). The result is shown in Table 15.

**Fig. 9** Process window for the form accuracy of  $0.5\ \mu\text{m}$ . **a** Packing pressure versus cooling time. **b** Mold temperature versus cooling time. **c** Mold temperature versus packing pressure. **d** Combination of three process parameters

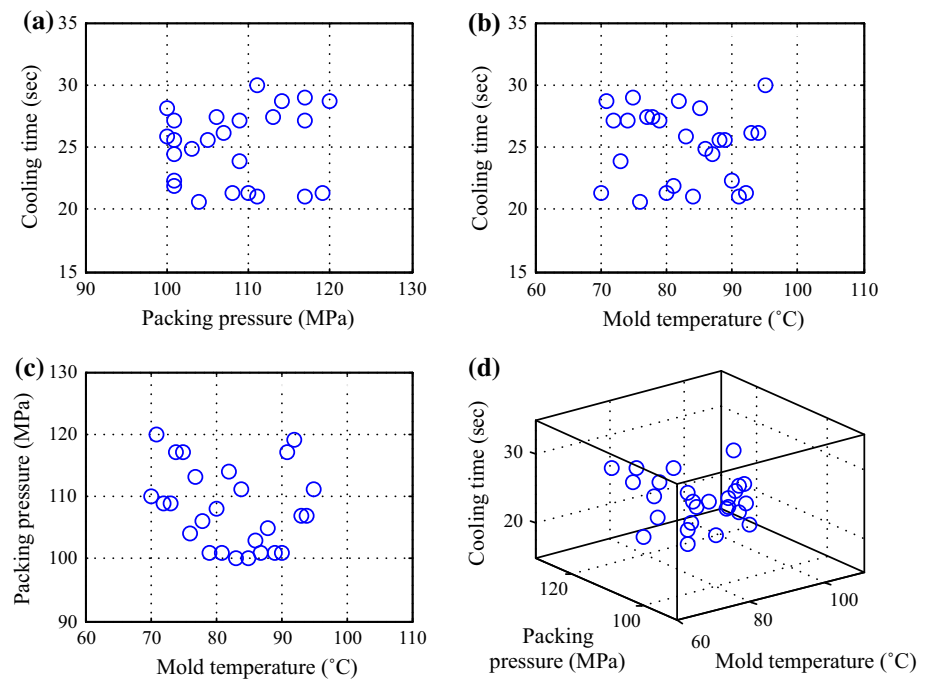
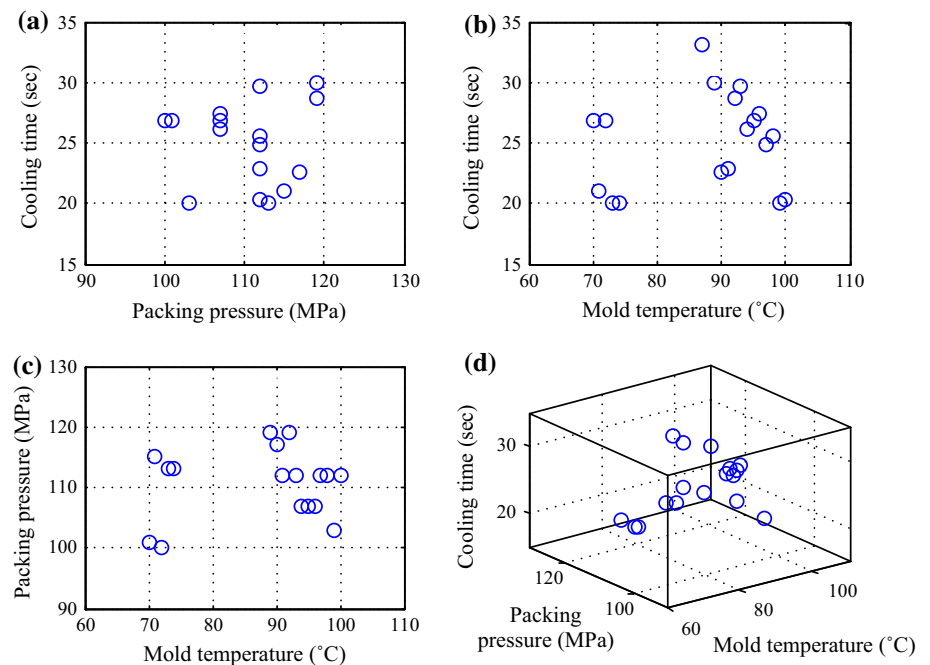


**Fig. 10** Process window for the form accuracy of  $0.7\ \mu\text{m}$ . **a** Packing pressure versus cooling time. **b** Mold temperature versus cooling time. **c** Mold temperature versus packing pressure. **d** Combination of three process parameters



The process parameters optimized by the GA were different from those based on the Taguchi Method, and the optimal form accuracy of the lens was better than that of the Taguchi Method, which was  $0.392\ \mu\text{m}$ . A confirmation experiment was conducted for this prediction result, and due to the experimental machine resolution, the process parameters optimized by the GA were simplified by rounding. According

to the experimental results, the measured lens form accuracy was  $0.415\ \mu\text{m}$ , and the error to the prediction value was 5.54%. Therefore, the process parameters optimized by the hybrid ANN and GA resulted in better lens form accuracy than the Taguchi experiment, and the form accuracy improved from  $0.479$  to  $0.415\ \mu\text{m}$ , for an improvement rate of 13.36%.

**Fig. 11** Process window for the form accuracy of 1  $\mu\text{m}$ . **a** Packing pressure versus cooling time. **b** Mold temperature versus cooling time. **c** Mold temperature versus packing pressure. **d** Combination of three process parameters

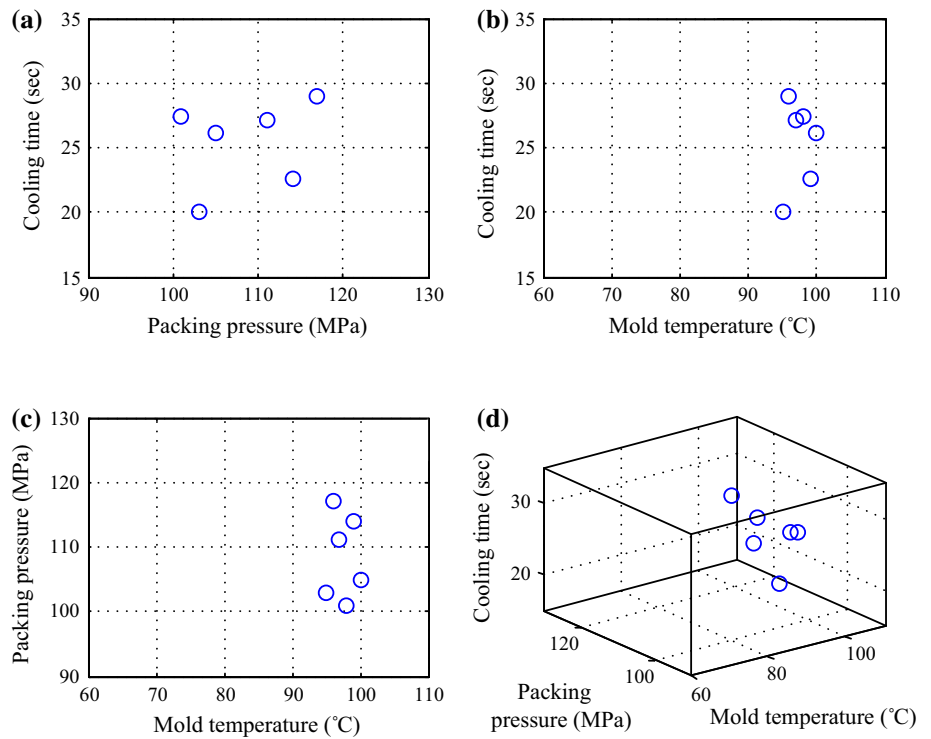


**Table 14** Confirmation experiment result for the inverse model

| Mold temp. | Packing press. | Packing time | Cooling time | Experiment avg | Target | Error (%) |
|------------|----------------|--------------|--------------|----------------|--------|-----------|
| 70         | 110            | 8.4          | 21.3         | 0.551          | 0.5    | 9.26      |
| 75         | 117            | 5.4          | 29           | 0.593          | 0.5    | 15.68     |
| 80         | 108            | 5.6          | 21.3         | 0.484          | 0.5    | 3.31      |
| 85         | 100            | 6.3          | 28.1         | 0.531          | 0.5    | 5.84      |
| 90         | 101            | 5.6          | 22.3         | 0.558          | 0.5    | 10.39     |
| 95         | 111            | 5            | 30           | 0.6            | 0.5    | 16.7      |
| 70         | 101            | 5            | 26.8         | 0.679          | 0.7    | 3.09      |
| 73         | 113            | 6.2          | 20           | 0.765          | 0.7    | 8.5       |
| 90         | 117            | 8.7          | 22.6         | 0.66           | 0.7    | 6.06      |
| 95         | 107            | 7.3          | 26.8         | 0.756          | 0.7    | 7.41      |
| 100        | 112            | 5.1          | 20.3         | 0.803          | 0.7    | 12.83     |
| 95         | 103            | 9            | 20           | 1.061          | 1      | 5.75      |
| 97         | 111            | 8.2          | 27.1         | 1.027          | 1      | 2.63      |
| 100        | 105            | 8            | 26.1         | 1.091          | 1      | 8.34      |
| Average    |                |              |              |                |        | 8.27      |

**Table 15** Confirmation experiment result for improved Taguchi optimal value using the GA

| Method             | Mold temp. (°C) | Packing press. (MPa) | Packing time (s) | Cooling time (s) | PV ( $\mu\text{m}$ ) |
|--------------------|-----------------|----------------------|------------------|------------------|----------------------|
| Taguchi experiment | 85              | 110                  | 7                | 25               | 0.479                |
| GA prediction      | 83.5484         | 117.4194             | 7.5806           | 29.3548          | 0.392                |
| GA confirm. exp.   | 84              | 117                  | 7.6              | 29.4             | 0.415                |

## Conclusion

This study used an ANN as the lens form accuracy prediction model, and employed a GA to inversely calculate the process parameters meeting the product quality requirements. This method enabled operators to rapidly obtain the optimal process parameters according to the required quality. The conclusions were as follows:

1. The results of ANOVA clearly showed that the mold temperature, packing pressure, and cooling time were the significant factors influencing lens form accuracy.
2. The ANN prediction model could successfully characterize the relationship between process parameters and lens form accuracy. The average error between the ANN prediction values and the experimental values was 4.89%, and the coefficient of determination was 0.9675.
3. The result indicated that the hybrid ANN and GA strategy was successful in determining the process parameters meeting the desired form accuracy of the lens in the injection molding in the case studies.
4. According to the results of the hybrid ANN and GA approach to improve the Taguchi optimal process parameters, better lens form accuracy could be obtained by using the proposed method. The form accuracy improved from 0.479 to 0.415  $\mu\text{m}$ , for an improvement rate of 13.36%.

**Acknowledgements** The authors are obliged to thank the National Science Foundation, Taiwan, ROC, for the Project fund (NSC100-2221-E-167-011).

## References

- Altan, M. (2010). Reducing shrinkage in injection moldings via the Taguchi, ANOVA and neural network methods. *Materials & Design*, *31*, 599–604.
- Ashhab, M. S., Breitsprecher, T., & Wartzack, S. (2014). Neural network based modeling and optimization of deep drawing: Extrusion combined process. *Journal of Intelligent Manufacturing*, *25*, 77–84.
- Chaulia, P. K., & Das, R. (2008). Process parameter optimization for fly ash brick by Taguchi method. *Materials Research*, *11*, 159–164.
- Che, Z. H. (2010). PSO-based back-propagation artificial neural network for product and mold cost estimation of plastic injection molding. *Computers & Industrial Engineering*, *58*, 625–637.
- Chen, C. P., Chuang, M. T., Hsiao, Y. H., Yang, Y. K., & Tsai, C. H. (2009a). Simulation and experimental study in determining injection molding process parameters for thin-shell plastic parts via design of experiment analysis. *Expert Systems with Applications*, *36*, 10752–10759.
- Chen, W. C., Fu, G. L., Tai, P. H., & Deng, W. J. (2009b). Process parameter optimization for MIMO plastic injection molding via soft computing. *Expert Systems with Applications*, *36*, 1114–1122.
- Chen, Z., & Turng, L. S. (2005). A review of current development in process and quality control for injection molding. *Advances in Polymer Technology*, *24*, 165–182.
- He, W., Zhang, Y. F., Lee, K. S., Fuh, J. Y. H., & Nee, A. Y. C. (1998). Automated process parameter resetting for injection moulding: A fuzzy-neuro approach. *Journal of Intelligent Manufacturing*, *9*, 17–27.
- Huang, C. N., & Chang, C. C. (2011). Optimal-parameter determination by inverse model based on MANFIS: The case of injection molding for PBGA. *IEEE Transactions on Control Systems Technology*, *19*, 1596–1603.
- Kamoun, A., Jaziri, M., & Chaabouni, M. (2009). The use of the simplex method and its derivatives to the on-line optimization of the parameters of an injection moulding process. *Chemometrics and Intelligent Laboratory Systems*, *96*, 117–122.
- Katherasan, D., Elias, J. V., Sathiya, P., & Noorul, Haq A. (2014). Simulation and parameter optimization of flux cored arc welding using artificial neural network and particle swarm optimization algorithm. *Journal of Intelligent Manufacturing*, *25*, 67–76.
- Kurtaran, H., Ozcelik, B., & Erzurumlu, T. (2005). Warpage optimization of a bus ceiling lamp base using neural network model and genetic algorithm. *Journal of Material Processing Technology*, *169*, 314–319.
- Kwak, T. S., Suzuki, T., Bae, W. B., Uehara, Y., & Ohmori, H. (2005). Application of neural network and computer simulation to improve surface profile of injection molding optic lens. *Journal of Material Processing Technology*, *170*, 24–31.
- Lau, H. C. W., Lee, C. K. M., Ip, W. H., Chan, F. T. S., & Leung, R. W. K. (2005). Design and implementation of a process optimizer: A case study on monitoring molding operations. *Expert System*, *22*, 12–21.
- Li, D., Zhou, H., Zhao, P., & Li, Y. (2009). A real-time process optimization system for injection molding. *Polymer Engineering & Science*, *49*, 2031–2040.
- Loera, V. G., Castro, J. M., Diaz, J. M., Mondrago'n, O. L. C., & Cabrera-R'ios, M. (2008). Setting the processing parameters in injection molding through multiple-criteria optimization: A case study. *IEEE Transactions on Systems, Man, and Cybernetics - Part C: Applications and Reviews*, *38*, 710–715.
- Mok, S. L., Kwong, C. K., & Lau, W. S. (1999). Review of research in the determination of process parameters for plastic injection molding. *Advances in Polymer Technology*, *18*, 225–236.
- Mok, S. L., Kwong, C. K., & Lau, W. S. (2000). An intelligent hybrid system for initial process parameter setting of injection moulding. *International Journal of Production Research*, *38*, 4565–4576.
- Mok, S. L., Kwong, C. K., & Lau, W. S. (2001). A hybrid neural network and genetic algorithm approach to the determination of initial process parameters for injection moulding. *International Journal of Advanced Manufacturing Technology*, *18*, 404–409.
- Mok, S. L., & Kwong, C. K. (2002). Application of artificial neural network and fuzzy logic in a case-based system for initial process parameter setting of injection molding. *Journal of Intelligent Manufacturing*, *13*, 165–176.
- Montgomery, D. C. (2001). *Design and analysis of experiments* (3rd ed.). New York: Wiley.
- Ozcelik, B., & Erzurumlu, T. (2005). Determination of effecting dimensional parameters on warpage of thin shell plastic parts using integrated response surface method and genetic algorithm. *International Communications in Heat and Mass Transfer*, *32*, 1085–1094.
- Ozcelik, B., & Erzurumlu, T. (2006). Comparison of the warpage optimization in the plastic injection molding using ANOVA, neural network model and genetic algorithm. *Journal of Material Processing Technology*, *171*, 437–445.
- Ozcelik, B. (2011). Optimization of injection parameters for mechanical properties of specimens with weld line of polypropylene using Taguchi method. *International Communications in Heat and Mass Transfer*, *38*, 1067–1072.

- Ross, P. J. (1996). *Taguchi techniques for quality engineering*. New York: McGraw-Hill.
- Sadeghi, B. H. M. (2000). A BP-neural network predictor model for plastic injection molding process. *Journal of Material Processing Technology*, 103, 411–416.
- Shen, C., Wang, L., & Li, Q. (2007). Optimization of injection molding process parameters using combination of artificial neural network and genetic algorithm method. *Journal of Material Processing Technology*, 183, 412–418.
- Taguchi, G., Chowdhury, S., & Wu, Y. (2005). *Taguchi's quality engineering handbook*. Hoboken: Wiley.
- Tang, C., Rohani, J. M., & Yajid, M. A. M. (2013). Characterization of green corrosion inhibitor using Taguchi dynamic approach. *International Journal of Electrochemical Science*, 8, 7991–8004.
- Yen, C., Lin, J. C., Li, W., & Huang, M. F. (2006). An abductive neural network approach to the design of runner dimensions for the minimization of warpage in injection mouldings. *Journal of Material Processing Technology*, 174, 22–28.
- Yin, F., Mao, H., & Hua, L. (2011). A hybrid of back propagation neural network and genetic algorithm for optimization of injection molding process parameters. *Materials & Design*, 32, 3457–3464.
- Zhu, J., & Chen, J. C. (2006). Fuzzy neural network-based in-process mixed material-caused flash prediction (FNN-IPMFP) in injection molding operations. *International Journal of Advanced Manufacturing Technology*, 29, 308–316.